Video Article

# Fractionation for Resolution of Soluble and Insoluble Huntingtin Species

Joseph Ochaba[1,2], Eva L. Morozko[2,3], Jacqueline G. O'Rourke[4], Leslie M. Thompson[1,2,3]

[1]Department of Psychiatry and Human Behavior, University of California Irvine

[2]UCI MIND, University of California Irvine

[3]Department of Neurobiology and Behavior, University of California Irvine

[4]Board of Governors Regenerative Medicine Institute, Cedars-Sinai Medical Center

Correspondence to: Leslie M. Thompson at lmthomps@uci.edu

URL: https://www.jove.com/video/57082
DOI: doi:10.3791/57082

Keywords: Biochemistry, Issue 132, Huntington's disease, aggregation, huntingtin, protein fractionation, insoluble, proteostasis

Date Published: 2/27/2018

Citation: Ochaba, J., Morozko, E.L., O'Rourke, J.G., Thompson, L.M. Fractionation for Resolution of Soluble and Insoluble Huntingtin Species. *J. Vis. Exp.* (132), e57082, doi:10.3791/57082 (2018).

## Abstract

The accumulation of misfolded proteins is central to pathology in Huntington's disease (HD) and many other neurodegenerative disorders. Specifically, a key pathological feature of HD is the aberrant accumulation of mutant HTT (mHTT) protein into high molecular weight complexes and intracellular inclusion bodies composed of fragments and other proteins. Conventional methods to measure and understand the contributions of various forms of mHTT-containing aggregates include fluorescence microscopy, western blot analysis, and filter trap assays.

However, most of these methods are conformation specific, and therefore may not resolve the full state of mHTT protein flux due to the complex nature of aggregate solubility and resolution.

For the identification of aggregated mHTT and various modified forms and complexes, separation and solubilization of the cellular aggregates and fragments is mandatory. Here we describe a method to isolate and visualize soluble mHTT, monomers, oligomers, fragments, and an insoluble high molecular weight (HMW) accumulated mHTT species. HMW mHTT tracks with disease progression, corresponds with mouse behavior readouts, and has been beneficially modulated by certain therapeutic interventions[1]. This approach can be used with mouse brain, peripheral tissues, and cell culture but may be adapted to other model systems or disease contexts.

## Video Link

The video component of this article can be found at https://www.jove.com/video/57082/

## Introduction

The disruption of protein quality control networks that ensure proper folding and degradation of cellular proteins is likely central to pathology in Alzheimer's disease (AD), Parkinson's disease (PD), Huntington's disease (HD), and other "protein misfolding" disorders[2,3]. A detailed understanding of the proteostasis network components and their contributions to pathology are therefore crucial to developing improved therapeutic interventions. HD is caused by the abnormal expansion of a CAG repeat within the HD gene resulting in an expanded stretch of polyglutamines (polyQ) in the huntingtin (HTT) protein[4]. A consistent pathological feature of HD pathogenesis is the resulting misfolding, accumulation, and aggregation of HTT in regions of the brain and in peripheral tissues, which has been shown to interfere in several ways with normal cell homeostasis and function[5,6]. While HTT is ubiquitously expressed, medium spiny neurons in the striatum are selectively vulnerable and most overtly affected with notable cortical atrophy also associated with HD pathogenesis.

The formation of aggregates of HTT in the brain of HD patients and animal models has typically served as a proxy marker for disease progression and dominant-negative gain of function for mHTT[7]. Although the precise mechanisms by which protein misfolding and aggregation may contribute to mHTT-induced toxicity remain unclear, the formation of these inclusions in the brain of HD patients and various animal models is an invariant and inevitable feature. Inclusions appear to be comprised largely of accumulated HTT fragments containing the N-terminal expanded polyQ, indicating that proteolysis and processing of full-length HTT as well as alternative splicing[8,9] may play an important role in the pathogenesis of HD. N-terminal HTT fragments may constitute a pathologic form of HTT that can aggregate rapidly, nucleate, and accelerate or propagate the aggregation process[10].

However, the presence of these inclusions does not necessarily correlate with HTT-induced toxicity or cell death[11]. HTT has been proposed to undergo an aggregation process from a soluble monomer through soluble oligomeric species and β-sheet fibrils to insoluble aggregates and inclusions[12]. Resolving these various protein species via standard biochemical assays has been a challenge in the field due to their stability in low-detergent lysis buffer and difficulty in visualizing using standard biochemical assays. Thus, methodological considerations are critical in detecting the degree and pattern of accumulated and aggregated mHTT.

The protocol presented here provides a method to visualize several intermediates of HTT, specifically the formation of an insoluble HMW HTT species that appears to closely track with HD pathogenesis and disease progression[1,13,14]. Being able to resolve and track multiple species of

 

mHTT provides researchers a biochemical tool to study disease pathogenesis and evaluate potential therapeutic interventions through their modulation and impact on disease pathogenesis.

## Protocol

Animal Ethics Statement - Experiments were carried out in strict accordance with the Guide for the Care and Use of Laboratory Animals of the National Institutes of Health and an approved animal research protocol by the Institutional Animal Care and Use Committee (IACUC) at the University of California, Irvine, an AAALAC accredited institution. All efforts were made to minimize animal suffering.

# 1. Preparation of Lysis Buffers

1. Prepare "Soluble" lysis buffer (10 mM Tris pH 7.4, 1% Triton-X 100, 150 mM NaCl, 10% glycerol) and sterile filter through 0.22 µm filter.
    1. For a working "Soluble" lysis buffer, measure N-Ethylmaleimide (NEM) and thoroughly dissolve in 100 mM phenylmethysulfonyl flouride (PMSF) dissolved in 100% EtOH.
    NOTE: Lysis Buffer Inhibitors: (i) 20 mM N-ethylmaleimide (NEM); (ii) 0.2 mM PMSF; (iii) 1 mM Sodium orthovanadate ($Na_3VO_4$); (iv) 1 µg/mL leupeptin; (v) 1 µg/mL aprotinin; (vi) 20 mM Sodium fluoride (NaF).
    CAUTION: Wear a face mask when working with NEM throughout the protocol. Working lysis buffer must be made fresh to ensure active inhibitors.
    2. For soluble lysis buffer with protease inhibitors, add inhibitors in the following order: Sodium Fluoride (NaF), up to volume with cold lysis buffer, Sodium orthovanadate ($Na_3VO_4$), Aprotinin, and Leupeptin.

2. For "Insoluble" lysis buffer, supplement to 4% SDS by adding 500 µL of 20% SDS to 2 mL of "Soluble" lysis buffer. Leave at room temperature.
    NOTE: SDS will precipitate out when kept at 4 °C ; keep this at room temp. Final Lysis Buffer composition: 10 mM Tris (pH 7.4); 1% Triton X-100; 150 mM NaCl; 10% glycerol; 4% SDS (Insoluble Only).

# 2. Soluble/Insoluble Fractionation Protocol

NOTE: See **Figure 1** for a schematic.

1. Label two sets of tubes for each sample: "Soluble" and "Insoluble."
2. Add X-µL of ice-cold working soluble lysis buffer supplemented with protease inhibitors (see 1.1.1) to tissue.
    NOTE: X = Volume varies depending on tissue amount; See **Table 1**.
3. For mouse brain tissue (*i.e.*, striatum), dounce slowly 30 times in glass 1 mL douncer and pipet into "Insoluble" labeled tube (keep on ice).
    NOTE: Be careful not to break surface of liquid after starting douncing, as bubbles will form and may yield incomplete homogenization.
4. For cells (*i.e.*, HeLa, HEK293T), rinse cells once with cold, 1x PBS. Remove PBS and apply minimal volume of lysis buffer to cells and lift with cell scraper.
    NOTE: For above cell lines, cells were plated at 5 x $10^5$ cells per 6 well plate and grown to near confluency. One well is comparable to volumes used for mouse striatum.
5. Transfer homogenate or cell lysate into labeled, "Insoluble" tubes and lyse on ice 1 h (Start clock after final tube is processed).
    NOTE: For cell lysates, triturate several times to break up cell clumps prior to starting incubation. Avoid formation of bubbles. Briefly vortex pulse each sample for 1 s halfway through lysing.
6. Centrifuge samples at 4 °C at 15,000 x g for 20 min.
7. Recover supernatant as the "Soluble" fraction.
    1. Remove with pipet, be careful not to disturb pellet/cloudy layer as this will contaminate the fraction. Pipet soluble fraction into "Soluble" labeled tube. Keep on ice.
8. Wash pellet with 500 µL of lysis buffer (x2) and centrifuge at 4 °C at 15,000 x g for 5 min after each wash; it is okay if some of the cloudy layer is pipetted off.
9. After final wash, remove ALL remaining wash buffer leaving only the tissue pellet.
    NOTE: From this point, insoluble samples should now be kept at room temperature.
10. Resuspend pellet with X-µL lysis buffer supplemented with 4% SDS (Volume can be adjusted depending on pellet size; see **Table 1**).
11. Sonicate each sample for 30 s at room temperature with a probe sonicator (125 Watts, 20 kHz, Pulse, Amplitude 40%, see **Table of Materials**).
12. Boil samples (rolling boil) for 30 min; Centrifuge briefly (15 s) at 6,000 x g as to not lose any sample.
13. Perform DC (detergent compatible) protein assay (see **Table of Materials**) or Lowry protein assay to measure protein concentration (recommended started dilutions of 1/5 of sample in respective lysis buffer for cell culture and 1/10 for tissue lysates).
    NOTE: Protein concentrations will have to be read using a DC or Lowry assay due to high detergent concentration.
14. Aliquot samples into 50 µL batches to avoid freeze-thaw issues.
    NOTE: Protocol can be paused here prior to further biochemical analysis by storing both fractions at -20 °C.

# 3. Western Blot and Quantification

1. Perform western blots as reported elsewhere[1,13] by diluting 30 µg of sample 1:1 in loading buffer (1.6x loading dye, 1x reducing).
    NOTE: 30 µg of protein per fraction is sufficient, but can be adjusted for optimal resolution. 3 - 8% Tris-Acetate poly-acrylamide gels should be used for the insoluble fraction. 4 - 12% Bis-Tris gels are recommended for the soluble fraction.
2. Boil samples (rolling boil) for 5 min. Centrifuge briefly (15 s) at 6,000 x g to collect sample.
3. Analyze fractions by SDS-PAGE and western blot, according to manufacturer's protocol for reduced samples.

NOTE: Insoluble fraction resolves best when transferred onto 0.45 µM nitrocellulose membrane. 0.45 or 0.2 µM nitrocellulose can be used for the soluble fraction, depending on the size of the protein of interest. Some optimization may be required for best transfer of HMW materials.

4. Stain membrane with whole protein stain (*e.g.*, MEMcode, see the **Table of Materials**) to visualize protein loading efficiency.
NOTE: Western blots can be analyzed by mean pixel intensity. Soluble fractions can be normalized to a house-keeping protein best suited for the experimental system. Insoluble fraction as relative protein abundance was verified by reversible protein staining or Histone 3 normalization on separate blot.

## Representative Results

Resolution of soluble and insoluble cell lysates following fractionation can be detected using western analysis and filter retardation assays (**Figure 2**). As an example, HEK293T cells were transfected using transfection reagent (*e.g.*, lipofectamine 2000), with HTT exon 1 encoding cDNA containing 97 glutamine repeats[15] followed by the poly proline rich region, and these cells were allowed to express for 44 h. Cells were treated with either 5 µM MG132 to block the proteasome or DMSO as a control for 18 h prior to harvest and lysed as described above. Following fractionation protocol, mutant HTT exon 1 resolves as a soluble monomer around 45 kDa on 4 - 12% Bis-Tris PAGE gels and as a HMW insoluble accumulated species on 3 - 8% Tris-Acetate PAGE gels (**Figure 2A**). Soluble monomer can be quantified and normalized to a house-keeping protein (shown here as GAPDH). HMW, insoluble mHTT is quantified as relative protein abundance by mean pixel intensity. When treated with the inhibitor MG132, there is a noticeable decrease in soluble monomer of mHTT along with a corresponding increase in HMW, insoluble mHTT.

Insoluble fractions can be analyzed by additional techniques such as a Filter Retardation assay to resolve insoluble, fibrillar mHTT[16] (**Figure 2B**). HeLa cells were similarly transfected as above with 97Q-HTT exon 1, and either His-SUMO-1 or His-SUMO-2. Cells were treated with either DMSO or MG132 for 18 h prior to fractionation and analyzed using western blot and filter retardation assays. Data shows that the presence of overexpressed SUMO isoform increases both HMW and fibrillary insoluble mHTT. Addition of MG132 exacerbates the increase in insoluble mHTT species. HWM mHTT species can also be modulated by overexpression or reduction of the HD disease target, PIAS1 in both HeLa cells[13] and mouse striata[1] (**Figure 2C-D**). Knockdown of PIAS1 in the rapidly progressing mouse model of HD, the R6/2, using viral delivery of an siRNA against PIAS1, reduces accumulation of HMW insoluble mHTT. Viral overexpression of PIAS1 in R6/2 mice leads to a notable increase in HMW insoluble mHTT (**Figure 2D**)[1]. The change in solubility between fractions is quantifiable and indicates that this protocol can track modulation of pathogenic mutant protein species, making this a suitable technique for pre-clinical biochemical assessments of disease intervention. Changes in insoluble, fibrillar species of mHTT also capture flux between protein species that is modulated by treatment with MG132 or regulation of potential therapeutic targets, such as PIAS1[1].

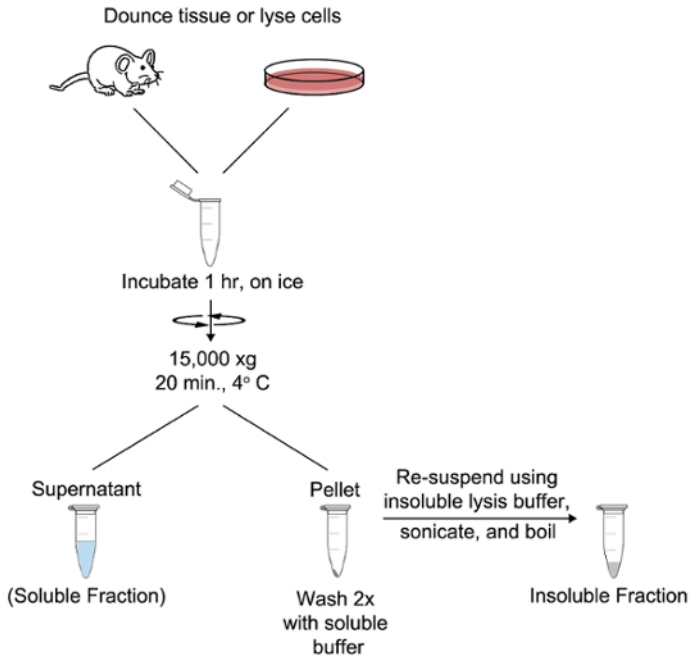


**Figure 1: Soluble/Insoluble fractionation protocol and protein resolution.** (**A**) Visual pipeline for fractionation protocol.The protocol described here can be applied to mouse tissue or cell culture samples but is suitable for adaption to other sample types. Please click here to view a larger version of this figure.

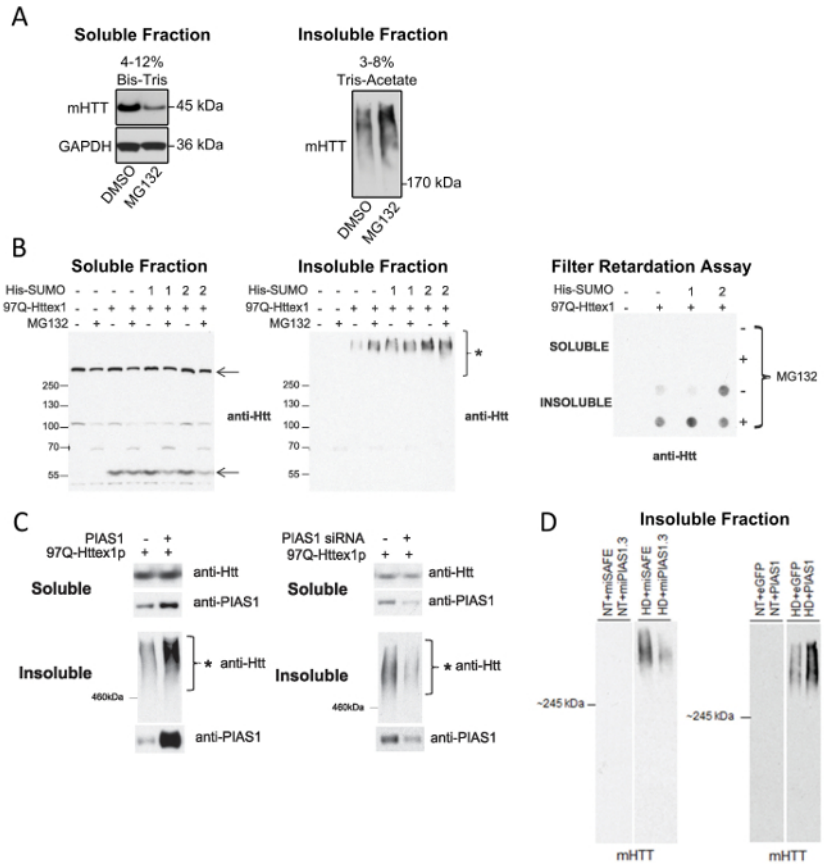


**Figure 2: Representative results for Soluble and Insoluble fractionations and analyses.** (**A**) Soluble and Insoluble fractions from HEK293T cell lysates resolved on a 4 - 12% Bis-Tris and 3 - 8% Tris-Acetate PAGE gels, respectfully. Soluble fraction normalized to GAPDH loading control shows fluctuation of mHTT exon 1 soluble monomer based on exposure to MG132. Insoluble fraction shows that HMW accumulated species of mHTT is also modulated by MG132 treatment. (**B**) Analysis of soluble and insoluble fractions from HeLa cell lysates using western blot and filter retardation analyses: HeLa cells were transfected with His-SUMO-1 or SUMO-2 and/or 97Q-HTT exon 1 and treated with 5 µM MG132 for 18 hr.* (**C**) Soluble and insoluble fractionation from HeLa cells overexpressing 97Q-HTT exon 1 and either overexpressed PIAS1 or treated with a siRNA against PIAS1 show regulation of HMW mHTT accumulation after modulating a potential therapeutic target.*(**D**) Insoluble fractions from mouse striata treated with microRNA against PIAS1 and resolved on 3 - 8% Tris-Acetate PAGE gels show modulation of HWM insoluble mHTT**. Panels (**B-C**) have been modified with permission[13]. Panel (**D**) has been modified with permission[1]. *Reprinted from O'Rourke *et al.*[13] with permission.**Reprinted from Ochaba *et al.*[1] with permission from Elsevier. Please click here to view a larger version of this figure.

| Tissue (per hemisphere) | Approximate weight (mg) | Volume Soluble (µL) | Volume Insoluble (µL) |
|---|---|---|---|
| mouse Striatum | 30 | 250 | 150 |
| mouse Cortex | 100 | 500 | 250 |
| mouse Hippocampus | 30 | 250 | 150 |
| mouse Cerebellum | 40 | 250 | 150 |
| mouse Skeletal muscle* | 100 | 300 | 150 |
| mouse Liver (lobe) | 100 | 400 | 200 |
| *connective tissue forms milky interface; remove to avoid contamination | | | |

**Table 1: Suggested volumes (X) for tissue-specific fractionation for both soluble and insoluble lysis buffers.** Insoluble lysis buffer volume based on starting amount of material, which can be adjusted accordingly based on insoluble pellet size.

## Discussion

Some precautions are needed for the above protocols to ensure consistent and quantitative results. First, mHTT in both fractions will spontaneously form aggregates over time upon multiple freeze thaw cycles, particularly when in a high concentration. It is thus critical to freeze aliquots of the protein preps, and thaw only the needed volume prior to running the assay as described in the protocol above. Further, if insoluble fraction yields white precipitant upon thawing, reconstitution may be necessary by an additional 5 s sonication pulse, 5 min boil, and re-quantitation prior to analysis via biochemical assays.

Quantitative resolution for this assay is achievable by normalizing mean pixel intensity of soluble fraction to that of a loading control or house-keeping gene within each sample. As shown here, GAPDH was used as a house-keeping gene for the soluble fraction as it predominantly localizes to the cytosol (**Figure 1**). Other commonly used house-keeping proteins are actin, α-tubulin, and Erk 1/2. However, suitable normalization proteins should be optimized for the system being studied to ensure steady state expression for accurate and uninfluenced normalization. While the insoluble fraction serves as a crude nuclear fraction as seen by presence of histone 3 and lack of GAPDH[1], resolution on 3 - 8% PAGE gels limits detectability to commonly used nuclear markers. Therefore, the insoluble fraction is suitable for quantification by using the raw signal intensity value as a relative representation of protein abundance. However, whole protein markers, such as reversible protein stains, are used to control for variations in protein loading and may be adapted as a normalization factor for insoluble fraction.

Additionally, while fractionation provides a means of resolving insoluble and soluble mHTT species, mHTT undergoes numerous conformational changes throughout disease pathogenesis, some of which will not be distinguishable in the insoluble fraction. Furthermore, some conformations may contribute beneficially towards disease outcome and act as stable clearance intermediates. It is therefore important to identify other mHTT conformers that correlate with outcomes for pathogenesis. Some optimization may be necessary to visualize other mHTT intermediates. To address this, SDS percentage can be increased to 20% if the aggregate is resistant to lower concentrations.

This protocol demonstrates protein fractionation conditions and resulting assays that detect various conformations and fragments of mHTT accumulation and aggregation in both cell culture and a transgenic mouse model of HD. This type of biochemical protein isolation is envisioned for assessment of disease progression in other HD models and may contribute to the growing understanding of mHTT dynamics within the cell and their impact on disease pathology.

After fractionation, samples can be processed in numerous ways. SDS-PAGE followed by western blot analysis will resolve soluble and insoluble mHTT species to provide a relative assessment on levels of mHTT species[1]. It is also possible to evaluate fractions in additional biochemical assays to further assess mHTT species. For instance, agarose gel electrophoresis (AGE) can resolve and detect soluble, oligomeric mHTT, while a filter retardation (FR) assay is a powerful tool to detect insoluble, fibrillary mHTT species[16,17].

An additional advantage this assay presents is the assessment of protein mislocalization associated with pathogenesis. As we demonstrated in [18], this fractionation protocol allows the visualization and tracking of proteins such as Rangap1, which appear to be sequestered by large insoluble aggregates and may not resolve on a standard PAGE gel. Additionally, as this assay also serves as a crude nuclear/cytoplasmic separation, one can also gauge mislocalization of proteins, *e.g.*, p65, in HD mouse models[1].

A prominent motivation for analysis of mHTT aggregation and accumulation is the development of novel HD diagnostics and therapeutics. Compounds that inhibit or reverse mHTT aggregation have been identified from high-throughput screens and targeted tests[1,12,19,20,21]. However, given the difficulty in resolving many of the forms of mHTT, evaluation of aggregation modulation has not always been feasible. Traditional lysis methods may dispose of pelleted cellular debris that potentially contain insoluble aggregate protein, or lysis buffers may not contain enough detergent for solubilization. The method described here provides a platform for isolating and detecting an aggregated form of mHTT that can be used as a biochemical marker in cell based or pre-clinical *in vivo* assessments.

The assays described here can be applied to other misfolded proteins. Due to the dynamic feature of misfolded proteins, these assays can be effectively coupled with other analyses to uncover in-depth mechanisms of protein homeostasis and aggregation. These analyses include measuring the steady state levels of aggregates and their partitions in different cell fractions (**Figure 1**) or analysis of protein folding/aggregation using purified recombinant proteins. These assays will help to distinguish direct or indirect effects of genetic or pharmacologic modulation on protein degradation or aggregation. Building on previous *in vitro* a-synuclein fractionated aggregation assessments[22], we have since applied this work to Parkinson's disease mouse models to resolve various conformations of a-synuclein[23]. Therefore, protocols described in this work may be applied to other models of protein misfolding and aggregation, and may contribute to the discovery and development of new therapeutics targeting aggregated proteins.

## Disclosures

The authors have nothing to disclose.

## Acknowledgements

This work was supported by the NIH (RO1-NS090390). We would also like to thank Dr. Joan Steffanfor technical assistance and discussion during the development of this assay.

## References

1. Ochaba, J. *et al.* PIAS1 Regulates Mutant Huntingtin Accumulation and Huntington's Disease-Associated Phenotypes In Vivo. *Neuron.* **90** (3), 507-520 (2016).
2. La Spada, A. R., & Taylor, J. P. Repeat expansion disease: progress and puzzles in disease pathogenesis. *Nat Rev Genet.* **11** (4), 247-258 (2010).
3. Reiner, A., Dragatsis, I., & Dietrich, P. Genetics and neuropathology of Huntington's disease. *Int Rev Neurobiol.* **98** 325-372 (2011).
4. A novel gene containing a trinucleotide repeat that is expanded and unstable on Huntington's disease chromosomes. The Huntington's Disease Collaborative Research Group. *Cell.* **72** (6), 971-983 (1993).
5. Sassone, J., Colciago, C., Cislaghi, G., Silani, V., & Ciammola, A. Huntington's disease: the current state of research with peripheral tissues. *Exp Neurol.* **219** (2), 385-397 (2009).
6. Weydt, P. *et al.* Thermoregulatory and metabolic defects in Huntington's disease transgenic mice implicate PGC-1alpha in Huntington's disease neurodegeneration. *Cell Metab.* **4** (5), 349-362 (2006).

7. Schulte, J., & Littleton, J. T. The biological function of the Huntingtin protein and its relevance to Huntington's Disease pathology. *Curr Trends Neurol.* **5** 65-78 (2011).
8. Gipson, T. A., Neueder, A., Wexler, N. S., Bates, G. P., & Housman, D. Aberrantly spliced HTT, a new player in Huntington's disease pathogenesis. *RNA Biol.* **10** (11), 1647-1652 (2013).
9. Neueder, A. *et al.* The pathogenic exon 1 HTT protein is produced by incomplete splicing in Huntington's disease patients. *Sci Rep.* **7** (1), 1307 (2017).
10. Arndt, J. R., Chaibva, M., & Legleiter, J. The emerging role of the first 17 amino acids of huntingtin in Huntington's disease. *Biomol Concepts.* **6** (1), 33-46 (2015).
11. Saudou, F., Finkbeiner, S., Devys, D., & Greenberg, M. E. Huntingtin acts in the nucleus to induce apoptosis but death does not correlate with the formation of intranuclear inclusions. *Cell.* **95** (1), 55-66 (1998).
12. Kim, S., & Kim, K. T. Therapeutic Approaches for Inhibition of Protein Aggregation in Huntington's Disease. *Exp Neurobiol.* **23** (1), 36-44 (2014).
13. O'Rourke, J. G. *et al.* SUMO-2 and PIAS1 modulate insoluble mutant huntingtin protein accumulation. *Cell Rep.* **4** (2), 362-375 (2013).
14. Shibata, M. *et al.* Regulation of intracellular accumulation of mutant Huntingtin by Beclin 1. *J Biol Chem.* **281** (20), 14474-14485 (2006).
15. Apostol, B. L. *et al.* A cell-based assay for aggregation inhibitors as therapeutics of polyglutamine-repeat disease and validation in Drosophila. *Proc Natl Acad Sci U S A.* **100** (10), 5950-5955 (2003).
16. Wanker, E. E. *et al.* Membrane filter assay for detection of amyloid-like polyglutamine-containing protein aggregates. *Methods Enzymol.* **309** 375-386 (1999).
17. Sontag, E. M. *et al.* Detection of Mutant Huntingtin Aggregation Conformers and Modulation of SDS-Soluble Fibrillar Oligomers by Small Molecules. *J Huntingtons Dis.* **1** (1), 119-132 (2012).
18. Grima, J. C. *et al.* Mutant Huntingtin Disrupts the Nuclear Pore Complex. *Neuron.* **94** (1), 93-107 e106 (2017).
19. Sontag, E. M. *et al.* Methylene blue modulates huntingtin aggregation intermediates and is protective in Huntington's disease models. *J Neurosci.* **32** (32), 11109-11119 (2012).
20. Trushina, E., Rana, S., McMurray, C. T., & Hua, D. H. Tricyclic pyrone compounds prevent aggregation and reverse cellular phenotypes caused by expression of mutant huntingtin protein in striatal neurons. *BMC Neurosci.* **10** 73 (2009).
21. Shahmoradian, S. H. *et al.* TRiC's tricks inhibit huntingtin aggregation. *Elife.* **2** e00710 (2013).
22. Kim, Y. M. *et al.* Proteasome inhibition induces alpha-synuclein SUMOylation and aggregate formation. *J Neurol Sci.* **307** (1-2), 157-161 (2011).
23. Goldberg, N. R. S. *et al.* Human Neural Progenitor Transplantation Rescues Behavior and Reduces alpha-Synuclein in a Transgenic Model of Dementia with Lewy Bodies. *Stem Cells Transl Med.* **6** (6), 1477-1490 (2017).


 